

## 31-P MR SPECTROSCOPY OF A LEG LYMPHANGIOSARCOMA

I.C. Kiricuta, R.G. Bluemm, H.W. Krawzak, J. Rühl, H.K. Beyer

Department of Radiation Oncology, University of Würzburg (IC), Institute of Radiology, Essen (RGB), Department of Surgery, Marienhospital, University of Bochum (HWK), Institute of Pathology, University of Bochum (JR), and Department of Radiology, Marienhospital Herne (HKB), Germany

*In a 64 year old man with a large, low grade lymphangiosarcoma of the right thigh, we correlated the results of in vivo 31-P-magnetic resonance spectroscopy (MRS), proton magnetic resonance imaging (MRI), and digital subtraction (DSA) with the pathologic specimen and histology. The 31-P MRS spectra of the tumor showed well-resolved peaks as follows: intense PCr (phosphocreatine), PDE (phosphodiester) and Pi (inorganic phosphate), and low PME (phosphomonoester). The Pi peak revealed an intratumor pH of 6.96 compared with 7.16 of normal skeletal muscle. The lower PME signal was consistent with low histopathologic mitotic activity of the tumor.*

Magnetic spectroscopy has been used to define further the metabolic activity and therapeutic response of a variety of tumors such as neuroblastoma, bone neoplasms, melanoma, brain cancers, and rhabdomyosarcoma (1-5). Magnetic resonance (MR) has also been demonstrated to be an accurate imaging technique characterizing tissue based on T1, T2 weighted relaxation times of the water protons (6,7). Interpretation of *in vivo* spectra is hampered, however, by discriminating between 31-P-MRS signals from tumors and those from adjacent normal tissues (8-10).

In this report, we correlated the *in vivo* findings of a well-resolved 31-P-MRS spectra with digital subtraction angiography (DSA), MRI and with the pathologic specimen and

histology in an adult patient with a large low-grade lymphangiosarcoma of the right thigh.

### CASE HISTORY

A 64 year old man noted an enlarging tumor of the right thigh for 18 months (*Fig. 1*). No metastatic disease was uncovered after computer tomography of the thorax and abdomen, bone marrow biopsy, and numerous biochemical and hematological blood screens.

### MRI

A 1.5 Tesla GE Signa whole-body imager (1m bore size) was used to obtain coronal T1-weighted and axial T2-weighted images of the right thigh before 31-P-MRS spectroscopic measurements and leg amputation (*Fig. 2a and 2b*).

### DSA

The right external iliac artery was catheterized via the left femoral artery and with crossover using the Seldinger technique. After 8cc Omnipac 300 was injected, the arterial and capillary phase images were depicted (*Fig. 3a and 3b*) by DSA (GE DS 5000 unit).

### Gross and Microscopic Pathology

The gross appearance of the large

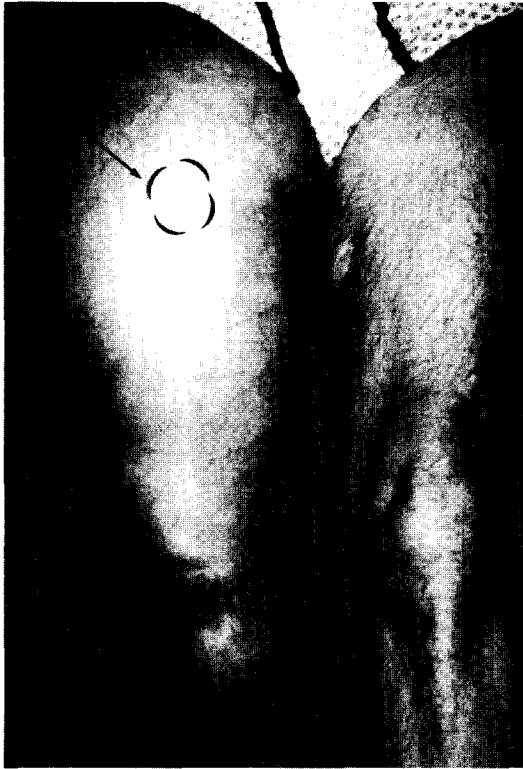


Fig. 1. Appearance of lymphangiosarcoma of the right thigh (arrow-circle indicates the position of the surface coil for acquisition of 31-P-MRS spectrum).

lymphangiosarcoma after leg amputation through the region from where the 31-P MR spectra were obtained is shown in Fig. 4a. A section above the knee is shown in Fig. 4b. Light microscopy showed a low grade malignant lymphangiosarcoma characterized by low mitotic activity, numerous microvessels with endothelial lining, capillary sprouts and broad areas of fibrosclerosis (Fig. 5a-c).

#### Surface Coil 31-P MRS Measurements

The intracellular phosphorous metabolites from the *in vivo* tumor mass in the right thigh (Fig. 6a) and of the uninvolved (normal) right gastrocnemius muscle (Fig. 6b) were monitored with an 8cm and 14cm diameter surface coil, tuned and matched to 24.84 MHz. The signal was localized to the tumor mass

mainly via coil placement. The magnetic field homogeneity was optimized by shimming using the proton signal of water. The acquired spectral data were analyzed on a GE-spectral analyzer, which includes baseline deconvolution and automatic spectral analysis. The repetition time TR was 2000msec.

The intracellular pH was measured from the chemical shift of the inorganic phosphate (Pi) peak, relative to PCr set at 0 ppm using the following formula:

$$K_{\text{obs}} = 3.22 + 2.51 / (1 + 10^{6.803 - \text{pH}}) \quad (10)$$

where  $K_{\text{obs}}$  is the observed chemical shift of the Pi signal (11).

#### RESULTS

The 31-P MRS spectrum of the uninvolved normal right gastrocnemius muscle is shown in Fig. 6b. The peaks represents PCr-phosphocreatine; Pi-inorganic phosphate, and  $\gamma$ ,  $\alpha$ ,  $\beta$  ATP-adenosintriphosphate signals. The spectrum of the lymphangiosarcoma was characterized by an intense PCr peak, low PME (phosphomonoesters) and moderate Pi and PDE (phosphodiester) (noted in Fig. 6a by X) peaks (Fig. 6b). The obtained spectrum is limited to the tumor mass as no normal muscle was found in the volume from where the 31-P-MRS spectrum was obtained (Fig. 4a). The PCr/ATP ratio of the lymphangiosarcoma was 2.5 which is considerably lower than 4.5 obtained for normal skeletal muscle. These ratios were calculated measuring the peak levels of the PME or -ATP seen in Fig. 6 and 6b.

From the 31-P MRS spectrum of the lymphangiosarcoma the measured chemical shift corresponded to a pH value of 6.96. The pH of normal skeletal muscle was 7.16.

#### DISCUSSION

Both MRI and 31-P MRS give valuable information on morphology and metabolic pathways of normal and tumor tissue (1,12).



Fig. 2. MRI of a lymphangiosarcoma of the right thigh. a) Midcoronal section through the largest diameter of the tumor (T1 weighted image TR=500msec, TE=20msec). Note the prolongation of T1 and the large tumor mass. b) Transverse section at the midpart of the thigh (T2 weighted image TR=2000msec, TE=80msec). Note the intact fascial lining and the increased signal intensity (arrow). The rest of the normal but atrophic muscle is barely outlined. Areas of inhomogeneity correspond to the gross specimen shown in Fig. 4.

31-P MRS spectra from deep-seated tumors are commonly affected by varying degrees of technical artifacts, chemical shifts and underlying structural contamination (8,9,13). In our patient, the 31-P-MRS spectrum of the thigh lymphangiosarcoma was free of contamination from normal tissues and specifically skeletal muscle. The 31-P-MRS

spectrum of the vascular tumor showed a low PME peak when compared with other malignant tumors (14). The PDE peak of the tumor was also intense when compared with other tumors. No PDE peak was detected in the normal gastrocnemius muscle (see Fig. 6b). PMEs are the byproducts of choline and ethanolamine kinases (the first steps in phospholipid synthesis), and also are substrates of glycerophosphorylcholine phosphodiesterase (the last step in phospholipid catabolism). Because the metabolic pathways to the formation of PMEs have not as yet been identified, their overall significance in tumor tissue remains speculative (2). Nonetheless, one might anticipate a close correlation between a low PME signal and low mitotic activity as shown by the histopathology (Fig. 5).

Griffiths et al (15) studying Walker 256 carcinosarcoma observed a 31-P MRS spectrum which contained little or no PCr, low PDE, relatively high Pi signals while the measured pH was 7.14. A large PME resonance was observed at the far-downfield end of the spectra.

In general, as the tumor enlarges, there is loss of PCr and nucleotide triphosphates (NTP) with concomitant increase in inorganic Pi and PME. These findings have been attributed to a relative decrease in blood supply. This explanation, however, is not valid for this patient's large well vascularized lymphangiosarcoma as displayed by the DSA (Fig. 3a and 3b). From a spectroscopic point of view, this tumor is characterized by large PCr and moderate Pi peak (Fig. 6a).

The Pi signal of the lymphangiosarcoma may be attributed to anerobic glycolysis with lactic acid as the end product and to low mitotic activity (Fig. 5). The intratumor pH of 6.96 is consistent with this explanation. Tumors exhibit remarkably heterogenous pH-distribution (16,17). Variability of single determinations may represent the sum of inter- and intra-tumor differences aside from a variance due to measuring (instrumental) inaccuracy. Griffiths et al (18) reported an *in situ* pH of 7.1 in an alveolar rhabdomyosarcoma.

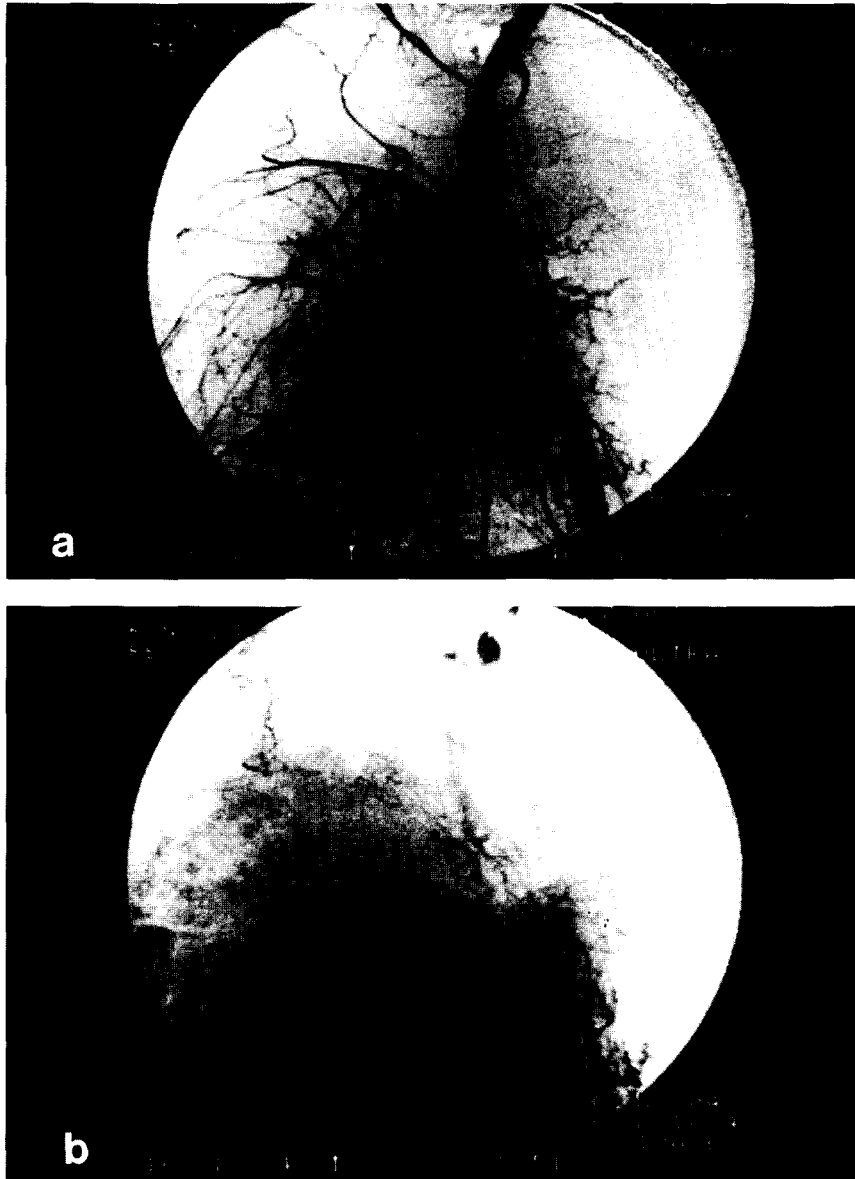


*Fig. 3. Digital subtraction angiography. a) Arterial phase (profunda femoris artery) showing the tumor vascularity. The superficial femoral artery is occluded. b) Tumor "blush" (capillary and parenchymal phase).*

The  $^{31}\text{P}$ -MRS spectrum of the lymphangiosarcoma showed an intense peak in the PDE region but not in normal skeletal muscle (*Fig. 6a and 6b*). Hitzig et al (19) have suggested that an additional signal in the PDE region represents a compound involved in high energy phosphate metabolism and may be a source of storage of high energy phosphate bonds. As our results suggest, perhaps the

large lymphangiosarcoma also uses such a compound to store high energy phosphate bonds. Alternatively, the phenomenon of high energy phosphate bond storage signifies adaptability of the tumor to less than optimum vascularity (19).

Elevated levels of PDE signals have been described in disorders other than malignancies such as Duchenne muscular dystrophy or in

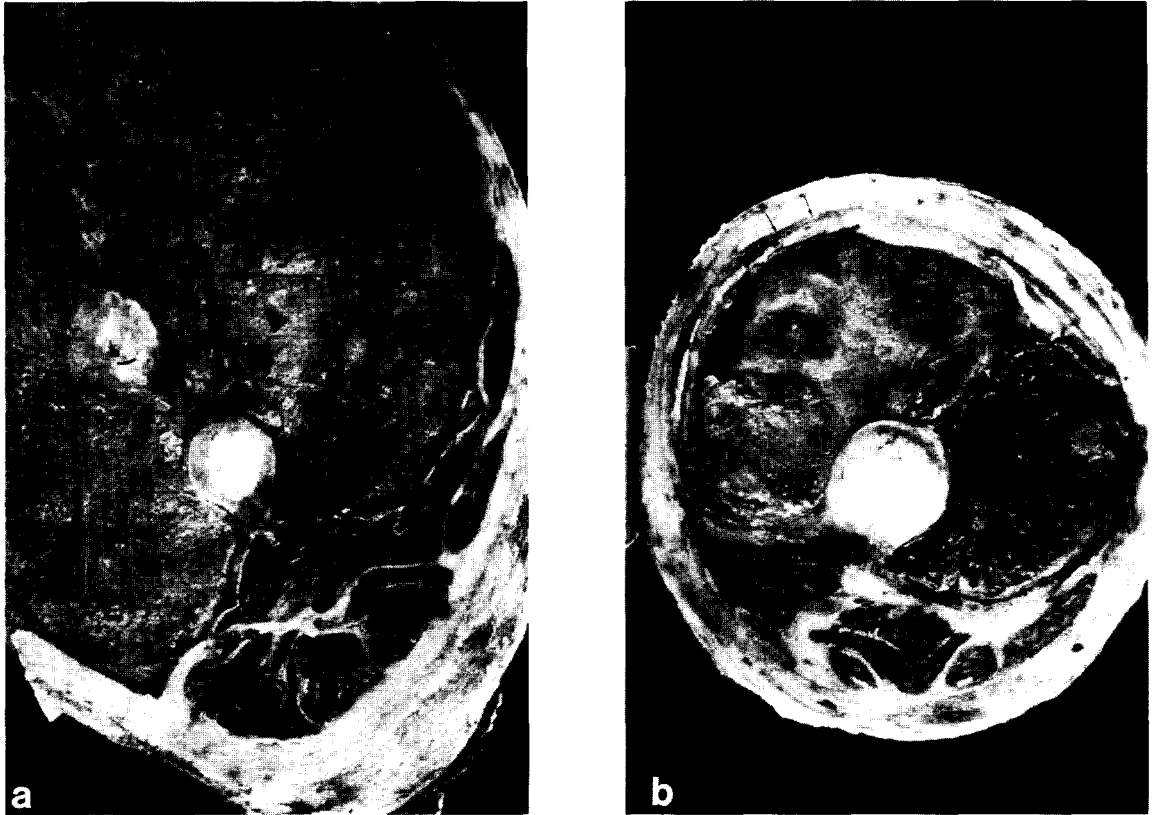


*Fig. 4. Resected specimen. a) Transverse section at the level of the center of surface coil through the lymphangiosarcoma. The area depicted by the arrowheads is where the  $^{31}\text{P}$ -MRS spectrum was acquired. Note atrophic muscle, proliferative tumor tissue, fibrosis and cavernous spongework of tumor and intact fascia (arrow). b) Transverse section above the knee at a distance from the spectroscopically investigated region. Note the thin atrophic muscle. The intact fascia is indicated by the arrow.*

skeletal muscle of elderly patients with degenerative arterial disease (2,4,14).

The neovascularity of this patient's lymphangiosarcoma is consistent with a high metabolic rate as demonstrated by  $^{31}\text{P}$ -MRS showing intense PCr and ATP peaks (*Fig. 6a*). The large relatively homogenous tumor mass and the extensive vascular supply shown by the DSA probably account for the intense PCr peak despite low mitotic activity and reflected spectroscopically by the low PME peak. The PME resonances may contain contributions from phosphorylethanolamine and phosphorylcholine, compounds involved in phospholipid synthesis. The PDE are their degradation productions (12). The PME

resonance may contain glycolytic intermediates of sugar phosphates, and this finding suggests that the tumor underwent glycolysis.

As a noninvasive technique  $^{31}\text{P}$ -MRS has potential scientific and clinical applications:

- 1) By defining a metabolite like PME the degree of tumor mitotic activity may be assessed.
- 2) Monitoring tumor pH signifies ongoing dynamics in the cell fraction of hypoxic or necrotic tumors.
- 3) Noninvasive measurement of intratumor pH before, during, and after antitumor therapy (e.g., radio-, chemotherapy, tumor necrosis factor, interferon) may be prognostic

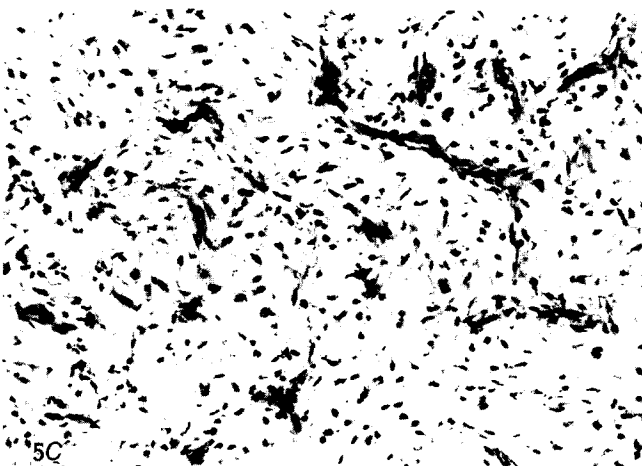
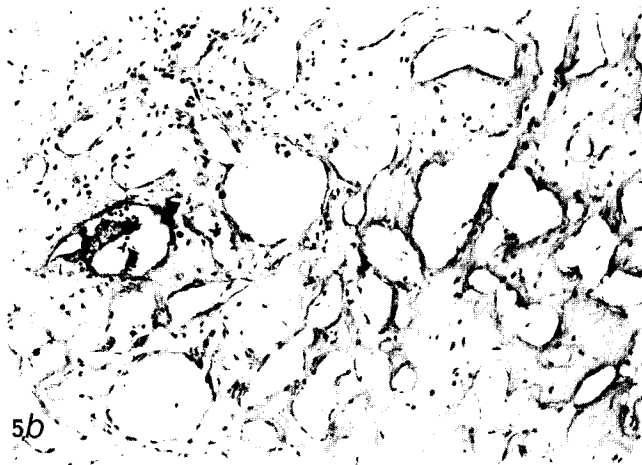


*Fig. 5. Light microscopic findings. a) Large communicating vascular spaces lined by endothelium. The lumina are filled with a light eosinophilic fluid, occasional lymphocytes but not erythrocytes. Another feature is myxoid elements with a lattice rich in capillaries (x60). b) Extensive fibrosclerosis with poorly interspersed cells between vascular spaces is seen (x100). c) Myxoid areas with rich branching capillaries without lipoblasts or mature adipocytes (x125).*

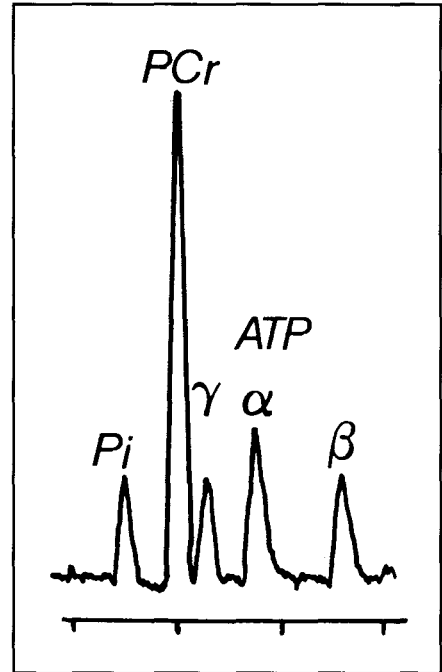
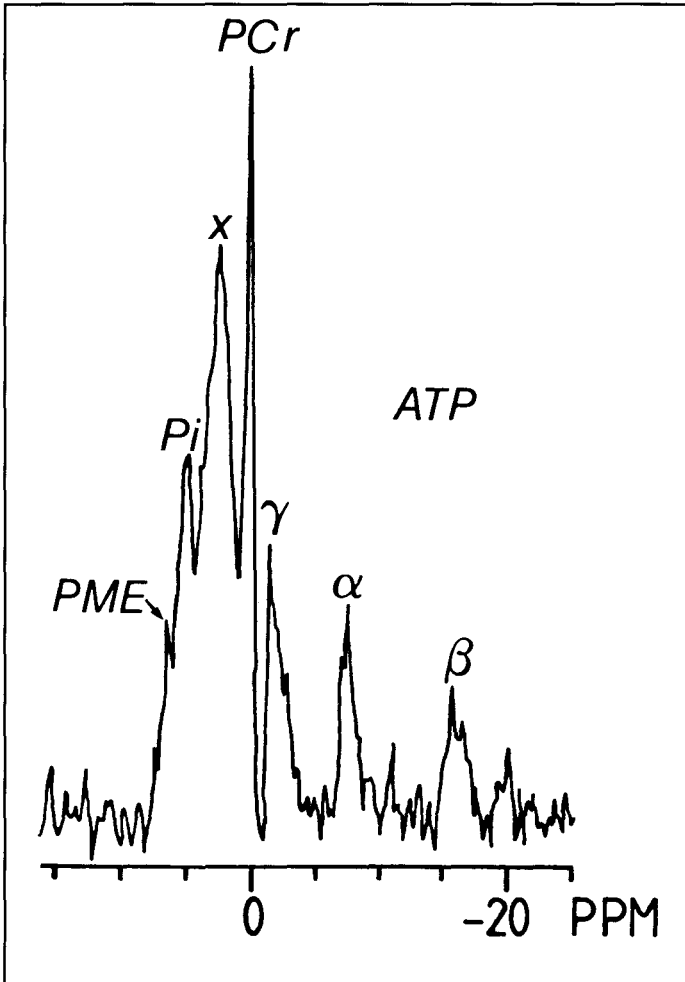


Fig. 6. *In vivo*  $^{31}\text{P}$ -MRS spectra of: left) low grade lymphangiosarcoma. Identification of resonances by chemical shift (Peak PME) — phosphomonoester; (Peak Pi) — inorganic phosphate; (Peak X) — phosphodiester; (Peak PCr) — phosphocreatine; ( $\gamma$ -Peak) —  $\gamma$  adenosinetriphosphate; ( $\alpha$ -Peak) — adenosinetriphosphate; ( $\beta$ -Peak) —  $\beta$  adenosinetriphosphate. upper right) Normal gastrocnemius muscle of the same patient.

especially with pH dependent treatment such as hyperthermia and chemotherapy.

Whereas the intratumor pH depends on a number of factors including blood supply, tumor growth fraction, doubling time, histology, and anatomic site, the value signifies the overall metabolic status. Tumors predominantly composed of hypoxic cells show an acid shift in pH typically lower than 7.0, whereas tumors with extensive necrosis display a more alkaline pH (>7.15-7.20).

#### REFERENCES

1. Cohen, JS: Phospholipid and energy metabolism of cancer cells, monitored by  $^{31}\text{P}$  MRS. Possible clinical significance. *Mayo Clin. Proc.* 63 (1988), 1199-1207.
2. Maris, JM, AE Evans, AC McLaughlin, et al:  $^{31}\text{P}$  NMR spectroscopic investigation of human neuroblastoma *in situ*. *N. Engl. J. Med.* 312 (1985), 1500-1505.
3. Naruse, S, K Hirikawa, Y Horikawa, et al: Measurements of *in vivo*  $^{31}\text{P}$  MR spectra in neuroectodermal tumors for the evaluation of the effects of chemotherapy. *Cancer Res.* 45 (1985), 2429-2433.
4. Ng, TC, AW Majors, T Meany: *In vivo* MR spectroscopy of human subjects with a 1.4T whole body MR imager. *Radiology* 158 (1986), 517-520.
5. Niedecker, AC, S Mueller, WP Aue, et al: Extremity bone tumors: Evaluation by  $^{31}\text{P}$  MR spectroscopy. *Radiology* 157 (1985), 167-174.

6. Kiricuta, IC, D Demco, V Simplaceanu: The state of water in normal and tumor tissues. *Arch. Geschwulstforsch.* 42 (1973), 214-216.
7. Kiricuta, IC, V Simplaceanu: Tissue water content and relaxation times in normal and tumor tissues. *Cancer Res.* 35 (1975), 1164-1167.
8. Meier, JE, D Flaming, WW Hunter, Jr., et al: Artifact reduction in low spacial resolution proton chemical shift images: A systematic analysis of phantom data. In: *Books of Abstracts, Society of Magnetic Resonance in Medicine, Vol. 2, Berkeley, CA; Society of Magnetic Resonance in Medicine, 1988, 935.*
9. Ordridge, RJ, A Connely, JAB Lohman: Image selected *in vivo* spectroscopy (ISIS): A new technique for spatially selected NMR spectroscopy. *J. Magn. Reson.* 66 (1986), 283-294.
10. Schmalbrock, P: Artifact reduction in low spacial resolution proton chemical shift images: A systemic analysis of phantom data (abstr.). In: *Book of Abstracts: Society of Magnetic Resonance in Medicine, Vol. 2, Berkeley, CA: Society of Magnetic Resonance in Medicine (1988), 395.*
11. Dhasmana, JP, SB Digerness, JM Gelcke, et al: The effect of adenosine deaminase inhibitors on the heart's functional and biochemical recovery ischemia: A study utilizing the isolated rat heart adapted to 31-P NMR. *J. Cardiovasc. Pharmacol.* 5 (1983), 1040-1047.
12. Daly, PF, RC Lyon, PJ Faustino, et al: Phospholipid metabolism in cancer cells monitored by 31-P NMR spectroscopy. *J. Biol. Chem.* (1987), 262:14875-14878.
13. Lawry, TJ, AA Twieg, AA Maudsley, et al: Computer simulation of MRS localization: Comparison of ISIS and spectroscopic imaging (SI) techniques. In: *Books of Abstracts, Society of Magnetic Resonance in Medicine, Vol. 2, Berkeley, CA; Society of Magnetic Resonance in Medicine, 1988, 944.*
14. Ng, TG, S Vijayakumar, A Majors, et al: Response of a non-Hodgkin lymphoma to Co-60 Therapy monitored by 31 P MRS *in situ*. *Int. J. Rad. Oncol. Biol. Phys.* 13 (1987), 1545-1551.
15. Griffiths JR, AN Stevens, RA Iles, et al: 31-P-NMR investigation of solid tumors in the living rat. *Biosc. Rep.* 1 (1982), 319-325.
16. Busse, J, W Müller-Klieser, P Vaupel: Intratumoral pH distribution—a function of tumor growth stage (abstract). *Pflügers Archiv.* 389 (1981), R55.
17. Gullino, PM, SH Clark, FH Crautham: The interstitial fluid of solid tumors. *Cancer Res.* 24 (1964), 780-797.
18. Griffiths, JR, E Cady, RHT Edwards, et al: 31-P NMR studies of a human tumor *in situ*. *J. Cell. Biol.* 95 (1983), 24-28.
19. Hitzig, BM, DC Johnson, E McFarland, et al: Unknown phosphate compounds in tail muscle of intact conscious newts by 31-P-NMR. *Comp. Biochem. Physiol.* 86 (1987), 537-540.

**Christian I. Kiricuta, M.D., Ph.D.**  
**Klinik und Poliklinik fHr Strahlentherapie**  
**Josef-Schneider-Strae 11**  
**8700 Würzburg, GERMANY**